Cellular/Molecular

Light Adaptation of Retinal Rod Bipolar Cells

Khris G. Griffis,[1,2] Katherine E. Fehlhaber,[1] Fred Rieke,[3] and Alapakkam P. Sampath[1]

[1]Department of Ophthalmology and Stein Eye Institute, David Geffen School of Medicine, University of California, Los Angeles, Los Angeles, California 90095, [2]Department of Integrative Biology and Physiology, University of California, Los Angeles, Los Angeles, California 90095, and [3]Department of Physiology and Biophysics, University of Washington, Seattle, Washington 98195

The sensitivity of retinal cells is altered in background light to optimize the detection of contrast. For scotopic (rod) vision, substantial adaptation occurs in the first two cells, the rods and rod bipolar cells (RBCs), through sensitivity adjustments in rods and postsynaptic modulation of the transduction cascade in RBCs. To study the mechanisms mediating these components of adaptation, we made whole-cell, voltage-clamp recordings from retinal slices of mice from both sexes. Adaptation was assessed by fitting the Hill equation to response-intensity relationships with the parameters of half-maximal response ($I_{1/2}$), Hill coefficient (n), and maximum response amplitude (R_{max}). We show that rod sensitivity decreases in backgrounds according to the Weber–Fechner relation with an $I_{1/2}$ of ~50 R^* s^{-1}. The sensitivity of RBCs follows a near-identical function, indicating that changes in RBC sensitivity in backgrounds bright enough to adapt the rods are mostly derived from the rods themselves. Backgrounds too dim to adapt the rods can however alter n, relieving a synaptic nonlinearity likely through entry of Ca^{2+} into the RBCs. There is also a surprising decrease of R_{max}, indicating that a step in RBC synaptic transduction is desensitized or that the transduction channels became reluctant to open. This effect is greatly reduced after dialysis of BAPTA at a membrane potential of +50 mV to impede Ca^{2+} entry. Thus the effects of background illumination in RBCs are in part the result of processes intrinsic to the photoreceptors and in part derive from additional Ca^{2+}-dependent processes at the first synapse of vision.

Key words: **adaptation; bipolar cell; calcium; retina; vision**

Significance Statement

Light adaptation adjusts the sensitivity of vision as ambient illumination changes. Adaptation for scotopic (rod) vision is known to occur partly in the rods and partly in the rest of the retina from presynaptic and postsynaptic mechanisms. We recorded light responses of rods and rod bipolar cells to identify different components of adaptation and study their mechanisms. We show that bipolar-cell sensitivity largely follows adaptation of the rods but that light too dim to adapt the rods produces a linearization of the bipolar-cell response and a surprising decrease in maximum response amplitude, both mediated by a change in intracellular Ca^{2+}. These findings provide a new understanding of how the retina responds to changing illumination.

Introduction

The visual system can encode light over an immense range of illumination. We see stimuli producing single-photon responses in a minority of the rod photoreceptors (Hecht et al., 1941; van der Velden, 1946; Baylor et al., 1979), but as light intensity increases, adaptation within the rods and in circuits that carry rod signals extends the dynamic range of rod vision to at least seven orders of magnitude (Dunn et al., 2006; Tikidji-Hamburyan et al., 2015; Frederiksen et al., 2021).

Rod bipolar cells (RBCs) are depolarizing (ON center) bipolar cells, which are the first point of pooling of rod signals in the mammalian retina. They allow convergence of up to 100 rods (Tsukamoto et al., 2001). The responses of RBCs are produced by a signal transduction mechanism that influences the gating of the transient receptor potential melastatin channel 1 (TRPM1), through action of a metabotropic glutamate receptor, mGluR6 (Morgans et al., 2009). The light-dependent opening of TRPM1 channels requires the deactivation of $G\alpha_o$ (Nawy, 1999; Dhingra et al., 2000; Okawa et al., 2010b), a process that is accelerated by the regulator of G-protein-signaling proteins RGS7 and RGS11 (Cao et al., 2012). All these steps in the mGluR6 cascade are potential points of modulation during light adaptation. The light-dependent TRPM1 inward currents have been shown to be

Received Mar. 10, 2023; revised Apr. 7, 2023; accepted May 2, 2023.

Author contributions: K.G.G., F.R., and A.P.S. designed research; K.G.G., K.E.F., and A.P.S. performed research; K.G.G. analyzed data; K.G.G., F.R., and A.P.S. wrote the paper.

This work was supported by National Institutes of Health–National Eye Institute Grants EY17606 (A.P.S.), EY29817 (A.P.S.), and EY0331 and NEI Core Grant EY00331 (UCLA), and Research to Prevent Blindness Unrestricted Funds to the University of California, Los Angeles Department of Ophthalmology. We thank Prof. Gordon L Fain for help with manuscript preparation.

The authors declare no competing financial interests.

Correspondence should be addressed to Alapakkam P. Sampath at asampath@jsei.ucla.edu.

https://doi.org/10.1523/JNEUROSCI.0444-23.2023

Copyright © 2023 the authors

affected by changes in internal calcium (Ca^{2+}) concentration (Shiells and Falk, 1999; Berntson et al., 2004; Nawy, 2004; Kaur and Nawy, 2012), although the mechanism of Ca^{2+} action and its role in setting the sensitivity of RBC responses with background light remain unclear.

To elucidate the processes responsible for adaptation of scotopic vision, we used whole-cell patch recordings in dark-adapted slices from rod photoreceptors and RBCs in darkness and in background light. Background intensities bright enough to adapt the rod photoreceptors caused changes in the sensitivity of RBCs that are mostly derived directly from rod adaptation. Light intensities too weak to produce significant adaptation in the rods can also altered the RBC response by mechanisms intrinsic to the bipolar cell. Dim backgrounds changed the sensitivity of the response to small differences in light intensity by linearizing the slope of the response-intensity curve, an effect likely mediated by entry of Ca^{2+}. Low background intensities also produce an additional novel form of adaptation that reduced the RBC maximum response amplitude (R_{max}), apparently by desensitizing some step in the RBC synaptic transduction cascade or by changing the conformation of the TRPM1 channels so that they become reluctant to open. This effect was also facilitated by calcium entry. These experiments provide new insight into the effects of exposure to background illumination on responses of retinal cells and the mechanisms of adaptation of scotopic vision.

Materials and Methods

Animals and animal care. This study was conducted in accordance with the recommendations of the *Guide for the Care and Use of Laboratory Animals* of the National Institutes of Health and the Association for Research in Vision and Ophthalmology Statement for the *Use of Animals in Ophthalmic and Vision Research*. The animal use protocol was approved by the University of California, Los Angeles, Animal Research Committee (Protocol ARC-2014–005). The primary method of killing was cervical dislocation. C57BL/6J mice (*Mus musculus*) were purchased from The Jackson Laboratory and were not screened for the absence of the rd8 mutation (Chang et al., 2002). All mice used in this study were between 2 and 6 months of age from approximately equal numbers of both sexes and were reared under a 12 h dark/light cycle.

Solutions. Retinal slices were made in HEPES-buffered Ames' medium (Sigma-Aldrich) containing 2.38 g L^{-1} HEPES balanced with 0.875 g L^{-1} NaOH to give an osmolarity of 284 ± 1 mOsm at pH 7.35 ± 0.05. This Ames-HEPES was kept on ice and bubbled continuously with 100% O_2. Bicarbonate-buffered Ames' medium (hereafter, referred to as buffered Ames' medium) was made from Ames' medium supplemented with 1.9 g L^{-1} $NaHCO_3$ and equilibrated with 95% O_2/5% CO_2, pH 7.4. The electrode internal solution contained the following (in mM): 125 K-aspartate, 10 KCl, 10 HEPES, 5 *N*-methyl-glucamine-HEDTA, 0.5 $CaCl_2$, 0.5 $MgCl_2$, 1 ATP-Mg, 0.2 GTP-Tris, 2.5 NADPH; pH was adjusted to ~7.3 with *N*-methyl-glucamine-OH, and the osmolarity was adjusted to ~280 mOsm. For experiments investigating effects of calcium buffering on RBC adaptation, the internal solution additionally contained 10 mM BAPTA (catalog #A4926, Sigma-Aldrich). All other constituents were identical to those of the normal internal solution.

Dissection and slice preparation. Mice were dark adapted for 12–20 h before the start of the experiment. All experiments began in the morning as defined by the vivarium dark/light cycle. Dissections were performed under infrared illumination ($\lambda \geq 900$ nm) with infrared image converters, either head mounted (ITT Industries) or dissecting-microscope mounted (B.E. Meyers). Following euthanasia, eyes from mice were enucleated, the anterior portion of the eye was cut, and the lens and cornea were removed. Eyecups were stored at 32°C in buffered Ames' medium in a light-tight container. Eyecups were bisected through the optic nerve head with a number 10 scalpel under the infrared-equipped dissection microscope (Carl Zeiss), and the retina was carefully removed from the retinal pigment epithelium with fine forceps. The isolated piece of retina was embedded in a low-temperature gelling agarose (3%; Sigma-Aldrich) in HEPES-buffered Ames' medium. Vertical retinal slices (200 μm in thickness) were cut in chilled, oxygenated Ames-HEPES with a vibrating microtome (VT-1000 S, Leica) and transferred either to a recording chamber or to the storage container for use later in the experiment. During recordings, the retinal slice was stabilized with a custom-made anchor of stainless steel (420 grade, polished), which was fastened to the recording chamber with a small amount of petroleum jelly. The slice was superfused with buffered Ames' medium at ~4 ml min^{-1}. The bath temperature was held at 36 ± 1°C by a temperature controller with feedback (catalog #TC-324B; Warner Instruments).

Physiologic recordings from rod photoreceptors and rod bipolar cells. Recordings from individual cells were made by whole-cell patch clamp from dark-adapted retinal slices as described previously (Arman and Sampath, 2010). Rods were visualized with illumination from an infrared light-emitting diode (LED; λ = 940 nm; Cairn Research) attached to the transmitted light path of the physiology microscope (Eclipse FN1, Nikon). Rod somata were identified by morphology and location in the outer nuclear layer (ONL), and RBC somata by morphology and location in the outermost portion of the inner nuclear layer as well as by their characteristic response to a flash. Some RBCs were filled with a fluorescent dye (100 μM; Alexa Fluor 750, λ_{max} = ~750 nm; Thermo Fisher Scientific) loaded in the recording pipette. Dye-filled cells were imaged following the recording with a Hamamatsu ORCAflash4.0LT+ (model C11440, Hamamatsu Photonics).

Filamented borosilicate-glass capillaries (BF120-69–10; Sutter Instruments) were pulled on the day of the experiment with a P-97 Flaming/Brown micropipette puller (Sutter Instruments) to a tip resistance in the bath medium of 15–19 MΩ for rods and 13–16 MΩ for RBCs. Cells were voltage clamped at holding potentials of −40 mV for rods and −60 mV or +50 mV for RBCs with an AxoPatch 200B patch-clamp amplifier (Molecular Devices). Series resistance of the recording pipette was compensated at 75–80% to prevent error in clamping potentials, and pipette capacitance was neutralized before break-in (Sherman et al., 1999). The patch seal was assessed after break-in, and recordings were terminated if the seal resistance was below ~1 GΩ, or the access resistance exceeded ~60 MΩ. All reported values of membrane potential have been corrected for liquid-junction potentials (Neher, 1992), which were estimated to be ~10 mV for our recording solutions (Ingram et al., 2019).

Recordings were low-pass filtered at 5 kHz by the patch-clamp amplifier and digitized at 10 kHz with a 16-bit A/D converter (ITC18/USB18, HEKA Elektronik). Data were collected in MATLAB (R2018b, MathWorks) with the open-source software package Symphony Data Acquisition System (https://symphony-das.github.io). All off-line data visualization and analysis was performed with custom scripts and the Iris DVA framework for MATLAB (Khris Griffis, https://github.com/sampath-lab-ucla/IrisDVA). Further zero-phase shift digital filtering was performed off-line with a seventh-order Butterworth filter and the MATLAB FilterM C Mex package. Typical filtering bandwidths were 0–30 Hz, and any deviations from this value for specific experiments are listed in the corresponding figure legends and below in Results.

Light stimulation. Stimuli were delivered with a dual OptoLED light stimulation system (Cairn Research) through a custom-built optical pathway that feeds into the transmitted light path of the physiology microscope. The stimulus and background LEDs had peak wavelengths of 505 ± 5 nm and 405 ± 5 nm. Light sources were attenuated by absorptive neutral-density filters (Thorlabs). At the beginning of each experiment, the microscope field-stop aperture was focused at the level of the slice to provide uniform illumination and was reduced to limit the stimulation region to a spot ~200 µm in diameter.

The intensities of the LEDs were measured with a calibrated photodiode (Gamma Scientific) through a photodiode amplifier (PDA200C, Thorlabs). Light intensities were calibrated as effective photons per square micrometer and adjusted for the absorption spectrum of rhodopsin (Govardovskii et al., 2000; Nymark et al., 2012). Stimulus intensities

were then converted to light-activated rhodopsins per rod (R^*) by accounting for the effective collecting area of a rod outer segment.

We estimated the effective collecting area of individual rods from the trial-to-trial variability in the responses to a fixed stimulus. Under the assumption that photon absorption obeys Poisson statistics, the mean number of photoisomerizations produced by the flash, $\bar{\eta}$, can be estimated by dividing the squared mean response by its variance, $\bar{\eta} = \bar{I}^2/\sigma_I^2$, where $\bar{I}^2$ is the average response and σ^2 is the variance produced by the flash (Field and Rieke, 2002). We calculated $\bar{\eta}$ from 4–6 flash intensities for 15 rods, and the collecting area was determined as the slope of the line relating $\bar{\eta}$ to the flash intensity. The average and 95% bias-corrected and accelerated (BC_a) confidence interval (see Experimental design and statistical analyses) of the collecting area was estimated to be 0.26 (0.14, 0.35) μm^2.

Response-intensity relationships. To calculate the normalized amplitude of the photoresponse to a given stimulus intensity, we correlated each response with a template generated from the average response across all flash intensities. We then took the amplitude relative to a baseline measured in the 200 ms before flash delivery (Sampath and Rieke, 2004). The amplitudes were scaled by the maximal response to the brightest flashes. This template-scaling procedure produced consistent estimates of the more variable dim-flash responses than measuring peak-current deflections. Response amplitudes were then related to flash intensities, Φ, with a Hill equation as follows:

$$\frac{R}{R_{max}} = \frac{1}{1+\left(\frac{I_{1/2}}{\Phi}\right)^n}, \quad (1)$$

where R is the response in pA, R_{max} is the maximum or saturating value of R to bright flashes, $I_{1/2}$ is the value of the stimulus intensity producing a half-maximal response, and n is the Hill coefficient.

To determine the effects of background light on maximum response amplitudes (R_{max}), responses to saturating flash intensities were recorded in the presence of a variety of background light intensities. These responses were bracketed by saturating flash responses recorded in darkness. A line was fit with respect to time between the peaks of the flashes in darkness, and the predicted maximal response, $\hat{R}_{max}$, was estimated to be the solution to the fit at the time of the peak measured in the presence of a background light. To measure the amount of suppression of the maximal response amplitude, the peak of the saturated response during the presentation of background light was divided by the predicted maximal response, $R_{max}/\hat{R}_{max}$. The predicted fractional response values were then related to background intensities, Φ_B, with an inverse Hill function. Parameters were estimated for initial offset, R_0; background intensity of half-maximal attenuation, $I_{1/2}{}^B$, and the Hill exponent, n, as follows:

$$\frac{R_{max}}{\hat{R}_{max}} = R_0 - \frac{\Delta R \Phi_B^n}{\left(I_{1/2}{}^B\right)^n + \Phi_B^n}. \quad (2)$$

In this equation, $\Delta R = R_0 - R_s$, and R_s is the settling point of the maximal attenuation. ΔR can then be taken as a metric for the maximal suppression of R_{max} by background light exposure (see Fig. 6).

Calculation of rod sensitivity. Rod sensitivity was measured from current responses to dim flashes of 505 nm light in whole-cell voltage clamp at a holding potential of −40 mV. Sensitivity (in pA R^{*-1}) was calculated in darkness and in the presence of background light as the peak amplitude of the response divided by the flash intensity for two to three flash intensities in the linear range of the rod photoreceptor. Mean sensitivities were scaled by those in darkness to give S_F/S_F^D, which was fit with the Weber–Fechner relation as follows:

$$\frac{S_F}{S_F^D} = \frac{I_0}{I_0 + I_B}, \quad (3)$$

where I_B is the background intensity and I_0 a constant sometimes called the dark light, which is the intensity of the background light required to reduce sensitivity by half.

Experimental design and statistical analyses. All uncertainties were calculated by Monte Carlo simulations (bootstrap) with 10,000 replicates except for time-series data, which instead used 2000 simulations in the interest of reducing computation time. Uncertainty is expressed as 95% confidence intervals about the mean. To increase accuracy and mitigate errors arising from the nonparametric situation, confidence intervals were estimated by the BC_a method (Efron, 1987).

In cases where fitting procedures were used, data were binned by logarithmic-spaced intervals, and fits were performed with a total least-squares method, also known as orthogonal regression, by the Total Least Squares Approach to Modeling Toolbox for MATLAB (Petráš and Bednárová, 2010). The fitting procedure was bootstrapped by resampling from the residuals of individual cells (Freedman, 1981; Efron and Tibshirani, 1986). The data were resampled, binned, and fit for 10,000 repetitions generating sampling distributions of model parameters. Uncertainty regions of the fitting parameters are presented as BC_a 95% confidence intervals. Uncertainty regions of the regression lines are the 95% confidence intervals generated from each bootstrapped fit over an interpolating region and they were displayed as a shaded region surrounding the fit traces. Statistical significance of fitting parameters, where applicable, was determined from the BC_a 95% confidence regions, which corresponds to a 5% α level ($p < 0.05$) (Efron and Tibshirani, 1986).

Statistical comparisons between BAPTA and control conditions for R_{max} experiments were made by first assessing a one-way repeated-measures ANOVA by a custom bootstrap approach for unbalanced design in MATLAB. This custom algorithm is equivalent to the standard linear mixed-effects model, except that bootstrap replicates are calculated from the residuals as the fixed-effects estimator (Freedman, 1981). *Post hoc* analysis proceeded if the results of ANOVA indicated a significant effect, that is, $p < 0.05$. Pairwise testing was performed on all pairs by a custom bootstrap algorithm of Welch's t test for unequal variances (Welch, 1938, 1947). To account for multiple testing errors, all p values were adjusted for false discovery rate (Benjamini and Hochberg, 1995). Sample sizes, N, are provided in Table 1 or in the Figure legends of corresponding experiments.

Results

Photoreceptor flash sensitivity is dependent on background light levels

Rod photoreceptors can detect single photons (Baylor et al., 1979), and rod-mediated vision operates over approximately seven orders of magnitude of light intensity. This requires substantial adaptation in rods and postrod retinal circuits. To identify rod photoreceptor contributions to adaptation under our experimental conditions, we used patch electrodes to record current responses to brief flashes of light that elicited no more than 20% of the maximal response in darkness and with increasing background light intensity (Fig. 1*A*, left). To measure flash sensitivities, the peak amplitudes of the current responses were divided by flash intensities (Fig. 1*A*, right). Sensitivity in background light was divided by sensitivity in darkness, and the resulting ratio was plotted as a function of background intensity (Fig. 1*B*). These changes in sensitivity agree with previous reports of background dependence of sensitivity in rod photoreceptors (Mendez et al., 2001; Makino et al., 2004; Woodruff et al., 2008; Chen et al., 2010; Morshedian and Fain, 2017), and we found a similar fit to the Weber–Fechner relation (Eq. 3). Our value of I_0 = 53 (40, 120) R^* s^{-1} agrees with previous measurements (Morshedian et al., 2018), although somewhat higher than reported by Mendez et al. (2001) or Dunn et al. (2006). Our data confirm a component of rod-pathway adaptation in the rods themselves that may be propagated through downstream circuitry.

Table 1. Response-intensity properties for RBCs

Background	Φ	$I_{1/2}$	*n*
$R^*sec^{-1}rod^{-1}$	R^*rod^{-1}	R^*rod^{-1}	
Dark [46]	0.015→120	1.3	1.7
		(1.2, 1.4)	(1.5, 1.9)
0.22 [3]	0.011→21	1.2	1.5
(0.17, 0.26)		(1.0, 1.6)	(1.2, 2.2)
0.5 [5]	0.03→71	1.3	1.3
(0.36, 0.62)		(1.0, 1.7)	(1.0, 2.5)
1.4 [4]	0.044→95	1.4	1.2
(1.2, 1.6)		(1.0, 1.9)	(0.89, 2.0)
2.8 [5]	0.022→84	1.5	1.0
(2.5, 3.1)		(1.2, 2.0)	(0.85, 1.3)
7.2 [5]	0.09→94	1.5	0.99
(5.1, 8.9)		(1.3, 1.9)	(0.85, 1.2)
18 [7]	0.051→220	1.8	1.1
(14, 23)		(1.5, 2.2)	(0.95, 1.5)
44 [5]	0.16 → 830	3.8	1.1
(36, 51)		(3.2, 4.7)	(0.92, 1.5)
110 [4]	0.058→420	4.0	1.1
(76, 130)		(3.4, 5.0)	(0.88, 1.4)
360 [5]	0.26→1000	7.8	1.0
(280, 430)		(6.4, 9.5)	(0.89, 1.2)
600 [3]	1.5→330	12	1.1
(600, 600)		(10, 13)	(0.92, 1.4)

Values are reported as means (95% BCa confidence interval) where applicable. The parameters $I_{1/2}$ and *n* were estimated from fitting Equation 1 with normalized response amplitudes that were elicited from specified stimulus intensity ranges, *Φ*, during constant illumination with the corresponding background intensity. Number of animals used are shown in brackets following the corresponding background mean intensity (left column).

Background light reduces nonlinearity of the rod bipolar light response

To characterize RBC adaptation, we measured current responses to brief flashes of light in slice preparations of dark-adapted retinas (Fig. 2). We identified RBC somata visually first by their location at the boundary of the inner nuclear layer and the outer plexiform layer, then by their characteristically large and rapid flash responses, and finally in a few experiments by filling cells with Alexa Fluor 750 added to the recording solution for morphologic verification at the end of the experiment (Fig. 2*A*). Response families to increasing flash intensities were recorded in a series of background intensities, and responses were averaged at each flash intensity and background (Fig. 2*B*, top to bottom). Flash intensity ranges used for each background are listed in Table 1.

We saw a clear reduction in maximal response amplitude with increasing background intensity, which was accompanied by an apparent acceleration of response decay. Further, we observed that the steepness of the relationship between flash intensity and response amplitude was reduced in dim backgrounds (Fig. 2*C*). It should be noted that unlike photoreceptors whose response decay can be adequately described by a first-order decay exponential (Chen et al., 2000), the decay of RBC flash responses is nonuniform across flash intensities and often displayed an oscillatory component. For this reason, we did not quantify a time constant of decay. Instead, we focused on the parameters of the relationship between response amplitude and flash intensity as measures of the effects of background light on RBC flash responses.

To characterize the properties of the RBC flash response, we fit a two-parameter Hill equation (Eq. 1) to normalized response amplitudes as a function of stimulus intensity. Response amplitudes for each cell were calculated from two to five repetitions of flash-intensity families that covered the dynamic range of the RBC response at every background light intensity (Table 1). Maximal responses decreased with increasing background light, falling from −320 (−410, −260) pA in darkness to −18 (−26, −11) pA in a steady background light of 600 $R^* s^{-1}$. To normalize response amplitudes to the range 0–1, amplitudes were scaled by the maximal response amplitude, R_{max}, on a cell-to-cell basis (Fig. 2*C*). We generated response-intensity curves from fitted parameters (Fig. 2*C*, smooth lines) and 95% confidence intervals (shaded regions) and show them for a selection of background intensities in Figure 2*C*. In dim backgrounds (producing fewer than ∼2 $R^* s^{-1}$; Fig. 2*C*, blue curve), we observed a flattening of the response-intensity curve accompanied by almost no shift in the $I_{1/2}$ parameter (Fig. 2*C*, compare black and blue curves). When the background intensity was increased to 50 $R^* s^{-1}$ (Fig. 2*C*, orange curve), a level at which rod sensitivity is reduced by half (Fig. 1*B*), the response-intensity curve was shifted to brighter intensities by about twofold while not appearing to flatten any further. In the brightest background intensities tested (600 $R^* s^{-1}$, Fig. 2*C*, green curve), the response-intensity curve shifted further to brighter intensities, reflecting an ∼10-fold decrease in sensitivity. Fitting parameters from all the backgrounds tested are given in Table 1.

The nonlinearity in the RBC response-intensity curve can be quantified by the Hill coefficient *n* (Sampath and Rieke, 2004). For rods, the response-intensity curve was best fit by Equation 1 with a Hill coefficient of one. For RBCs, the Hill coefficient was much larger in darkness. Fitting Equation 1 to the RBC responses in darkness yielded estimates of $n = 1.7$ (1.6, 1.9) and $I_{1/2} = 1.3$ (1.2, 1.4) R^*. Increases in background intensities that were too dim to desensitize rods, that is, producing fewer than ∼3 $R^* s^{-1}$, markedly flattened the response-intensity curve, reducing *n* to 1.0 (0.89, 1.3) for a 2.8 $R^* s^{-1}$ background ($p < 0.05$ by 95% CI comparison). Note that over the same background regime, the dimmest flashes on average elicited a greater fractional response, and responses to near-saturating flashes were slightly compressed (Fig. 2*C*, compare blue to black plots). For visual comparison, *n* parameter fits are plotted against background intensities in Figure 3*A*. These results show that relief of nonlinearity occurs at background intensities too dim to elicit changes in rod sensitivity (Fig. 1*B*).

To estimate changes in RBC flash sensitivity apart from the change in nonlinearity, we took the inverse of the $I_{1/2}$ parameter as a measure of sensitivity. We then scaled this value by the value of $I_{1/2}$ in darkness and took this ratio as an estimate of S_f/S_f^D for the bipolar cell. These values were averaged and plotted as a function of background intensity in Figure 3*B*. RBC sensitivity declined with increases in background intensity in the same regime as rod sensitivity (Fig. 1*B*). To compare changes in RBC flash sensitivity to sensitivity in rod photoreceptors, we overlaid the Weber–Fechner relationship from the rod experiments (Fig. 3*B*, red curve; with $I_0 = 53$ $R^* s^{-1}$). The decline in RBC flash sensitivity remarkably paralleled the change in rod sensitivity observed during rod adaptation. These data indicate that rod adaptation has a direct influence on the flash sensitivity of RBCs during rod-bipolar adaptation.

This rod adaptational influence appears at backgrounds brighter than those that produce the relief in nonlinearity. These observations support the hypothesis that the response-intensity nonlinearity is postsynaptic in origin (Sampath and Rieke, 2004; Okawa et al., 2010a) and that RBC sensitivity may be imparted by rods at brighter background light intensities. Together, our results suggest a mechanism of adaptation separate of rod adaptation that is intrinsic to RBCs (see below, Discussion).

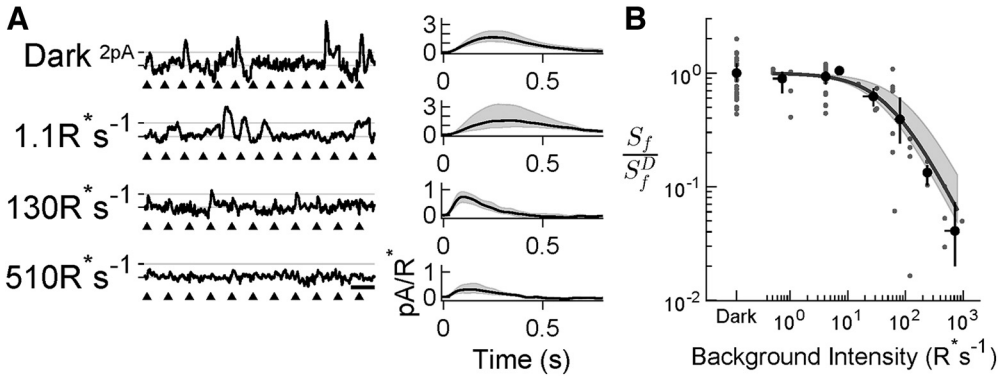

Figure 1. Dim flash responses are sped and reduced in amplitude by background light. ***A***, Representative patch-clamp current records ($V_m = -40$ mV) from dark-adapted C57BL/6J rods in darkness (0 R* s^{-1}), and background intensities of 1.1, 130, and 510 R^* s^{-1}. Flashes of fixed intensity were delivered as indicated by the arrowheads. Time scale bar is 200ms, gray horizontal lines indicate 2pA. Left, Averaged gain from two to three flash intensities corresponding to the background intensities in ***A***. ***B***, Sensitivity decreases as a function of background intensity. The reduction in sensitivity follows a Weber–Fechner relationship (Eq. 3), which describes a background intensity, 53 (40, 120) R^* s^{-1}, where sensitivity is decreased by half.

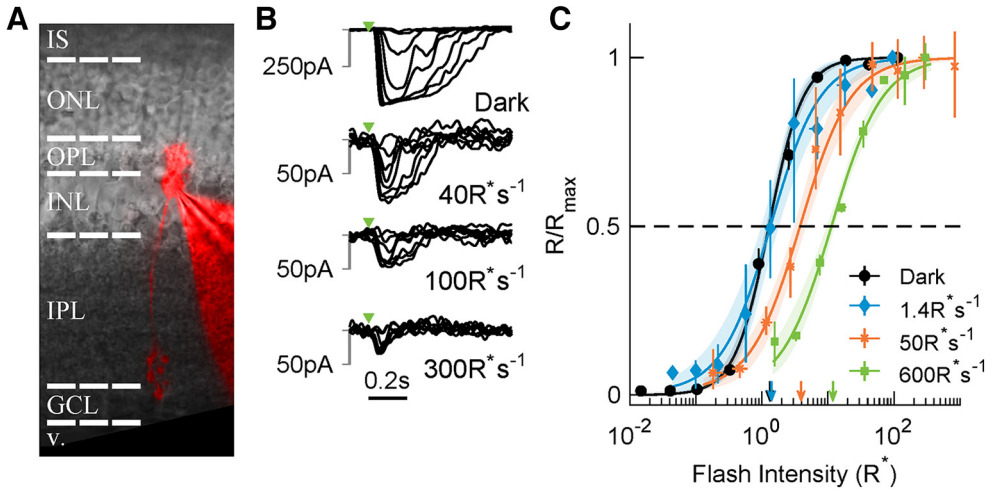

Figure 2. RBC responses in background light. ***A***, Rod bipolar cells (filled with Alexa 750 dye, red) were recorded from retinal slices using whole-cell patch configuration in voltage-clamp mode ($V_m = -60$ mV). ***B***, RBC current responses to brief flashes of light delivered as indicated by the green arrowhead (from top to bottom) in darkness [$R_{max} = -320$ (−400,−260) pA] and in the following background illuminations: 18 R^* s^{-1} [$R_{max} = -81$ (−120, −48) pA], 40 R^* s^{-1} [$R_{max} = -43$ (−57, −30) pA], and 300 R^* s^{-1} [$R_{max} = -25$ (−31, −20) pA]. Filter bandwidth, 0–50 Hz. R_{max} values are given as mean (95% BCa confidence intervals). ***C***, Normalized response amplitudes as a function of flash intensity in darkness (black) and background illuminations of 1.4 R^* s^{-1} (blue), 51 R^* s^{-1} (orange), and 600 R^* s^{-1} (green). Normalized response amplitudes were fit with a Hill equation (Eq. 1; smooth lines). A selection of all background intensities recorded from are shown (Table 1, complete list). As background light intensity increased, first, a flattening of the response-intensity curve was observed (blue), which corresponded to a decrease in the *n* parameter from 1.6, in darkness to ∼1 by 10 R^* s^{-1} (Fig. 3). Then a rightward shift in the $I_{1/2}$ parameter from 1.3 (1.2, 1.4) R^* in darkness (black arrow) to 3.8 (3.2, 4.7) R^* in a background light of 44 (36, 51) R^* s^{-1} (orange arrow), and 12 (10, 13) R^* in a 600 R^* s^{-1} background light (green arrow). IS, Inner segment; OPL, outer plexiform layer; INL, inner nuclear layer; IPL, inner plexiform layer; GCL, ganglion cell layer; v., vitreous.

Calcium modulates RBC nonlinearity

To study the effects of calcium on RBC adaptation, we filled the recording pipette with a solution containing 10 mM of the fast calcium chelator BAPTA (see above, Materials and Methods). BAPTA buffering has been shown to reduce transient peaks of the RBC light response and increase nonlinearity of the response-intensity curve (Berntson et al., 2004). We recorded flash response families from RBCs in darkness (Fig. 4*A*) and generated a response-intensity curve from nine cells (Fig. 4*B*). Confirming prior reports, we found a slight increase in sensitivity, that is, a reduction in $I_{1/2}$ [$I_{1/2}$ = 0.9 (0.79, 1.1) R^*, $p < 0.05$ by 95% CI comparison], and a strong increase in nonlinearity [n = 2.3 (1.9, 2.4) R^*, $p < 0.05$ by 95% CI comparison]. In contrast to previous reports with application of 10 mM BAPTA, we did not observe a significant difference in averaged maximal responses in darkness [−330 (−480, −230) pA] compared with control conditions [$R_{max} = -320$ (−400,−260) pA]. This discrepancy may result from differences in recording solutions. Because Ca^{2+} entry during the light response is facilitated by TRPM1 channels in the RBC dendrite (Nawy, 2000), these results suggest that Ca^{2+} entry plays a role in adjusting the linearity of the response.

Background light decreases the RBC maximal response

In the whole-cell patch configuration, RBC flash responses decrease in amplitude over a time span of 1–2 min following break-in. The reason for this rundown is unknown. We found that by decreasing the size of the recording electrode to resistance values of ∼16 MΩ, we could extend the duration of responsiveness by more than a minute. We characterized the rundown in our slice preparations in preliminary experiments, where we repeatedly delivered saturating flashes in darkness. We found that the maximal response amplitude slowly decreased in a linear trend over time, in agreement

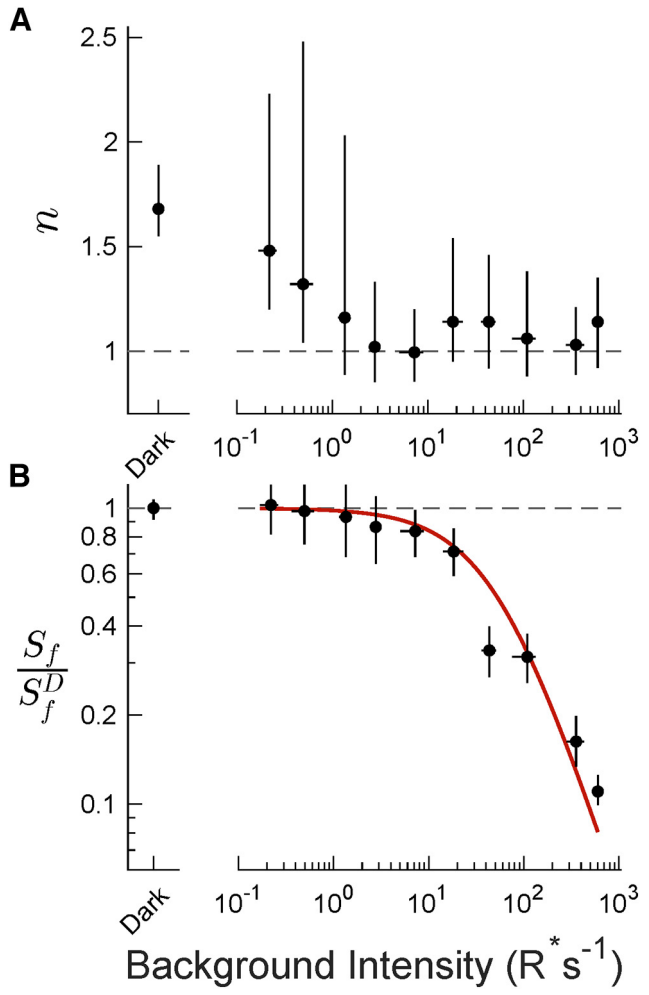

Figure 3. Hill fit parameters for RBC response-intensity relationships. ***A***, Hill coefficients as a function of background intensity. Points indicate means, and lines indicate BCa 95% confidence intervals. Dashed line at $n = 1$ represents complete relief of nonlinearity. ***B***, RBC sensitivity scaled by sensitivity in darkness as a function of background intensity. Sensitivity was taken as the inverse of the $I_{1/2}$ parameter. The dashed line in ***B*** indicates sensitivity in darkness of 1/(1.7 R*). For comparisons, we show in red the Weber relation from the reduction in rod photoreceptor gain with I_0 = 53 (40, 120) R*s^{-1} (Fig. 1*B*, smooth line). RBC sensitivity appears to have a similar background dependence as that of rod gain.

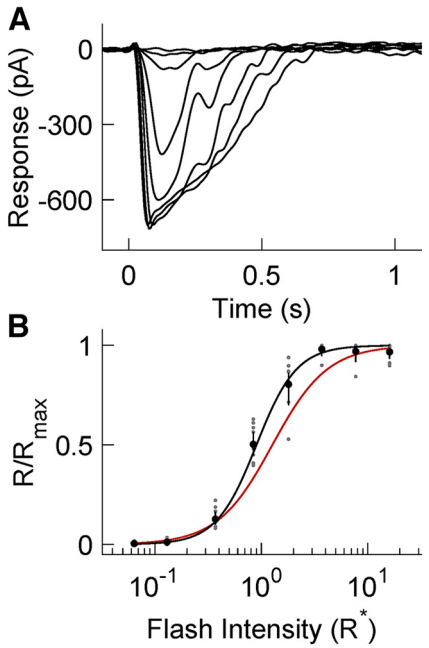

Figure 4. Dialysis of 10 mM BAPTA increases nonlinearity in darkness. ***A***, Representative RBC responses with 10 mM BAPTA loaded in the recording pipette. Current responses, in voltage clamp (Vm = −60 mV), to 10 ms flashes of the following intensities: 0.064, 0.13, 0.37, 0.84, 1.8, 3.7, 7.7 and 16 R*. ***B***, Normalized response amplitudes for nine cells (black points) fit with Equation 1 (black curve) compared with the Hill fit from control cells (red curve). Hill fit parameters for BAPTA-loaded cells were $I_{1/2}$ = 0.9 (0.79, 1.1) R* and n = 2.3 (1.9, 2.4). Averaged maximal responses (R_{max}) in darkness were −330 (−480, −230) pA. Uncertainties are expressed as means with BCa 95% confidence intervals in parentheses.

with similar measurements made in dogfish ON bipolar cells (Shiells and Falk, 1999) and tiger salamander RBCs (Nawy, 2004), albeit on a faster time course. From these results, we devised a protocol to study maximal response amplitudes in mouse RBCs that mitigated the effects of rundown.

The experiment was conducted as shown in Figure 5*A*. To verify that R_{max} amplitude attenuation was because of background light and not rundown, we recorded maximal responses in darkness and in background light from the same cell. A saturating flash was delivered in darkness (intensity 1), and the cell was allowed to recover to baseline. A background light was then turned on and held constant for 8–10 s before a second saturating flash was delivered (intensity 2); the brightness of the second flash was determined from response-intensity curves like those in Figure 2 and Table 1. The background light was turned off, and the cell was allowed another 8–10 s to adapt to darkness. A final saturating flash was then given (intensity 1) before terminating the experiment. Assuming a linear decrease of the maximal response, we fit a line to the peaks in the bracketing dark responses with respect to time (Fig. 5, dashed lines). Using the parameters of these linear fits, we calculated the expected maximal response peak at the time of the measured peak of the response in background light.

As the background light level was increased, the maximal response peak was smaller than predicted (compare peaks at stimulus 2 to corresponding dashed lines). This effect is especially evident for the brightest background of 300 R* s^{-1}, where the initial response to the background light corresponded closely to the predicted maximum given by the dashed line, but the response in the presence of the background to a saturating flash fell far short of this prediction. A full flash series at this 300 R* s^{-1} background level is given in Figure 2*B*, where it is evident that the response saturates at a much smaller value of R_{max} than in the absence of a background. The RBC in background light behaves as if steady illumination modulates a step in the RBC transduction cascade so that the number of Gα_o available to be deactivated or the proportion of TRPM1 channels available to open decreases.

To characterize the relationship between background intensity and attenuation of the maximal response, we took the ratio of the recorded response peaks in background light, R_{max}, as a fraction of the predicted maximum, $\hat{R}_{max}$. The fractional maximum responses, $R_{max}/\hat{R}_{max}$, are plotted in Figure 6 as the black symbols and have been fitted with an inverse Hill function (Eq. 2, Fig. 6*C*, black line). We found consistent and large decreases in $R_{max}/\hat{R}_{max}$ at background intensities below 10 R* s^{-1}; $R_{max}/\hat{R}_{max}$ at these dim intensities was significantly >1.0 at $p = 3 \times 10^{-5}$ (ANOVA). A background producing only 2.5 R* s^{-1} decreased the maximum response relative to that in darkness by 10%, corresponding to a response peak of −280 (−420, −190) pA. Decreases in $R_{max}/\hat{R}_{max}$ at these background intensities could not have been produced by adaptation in the rods, which is

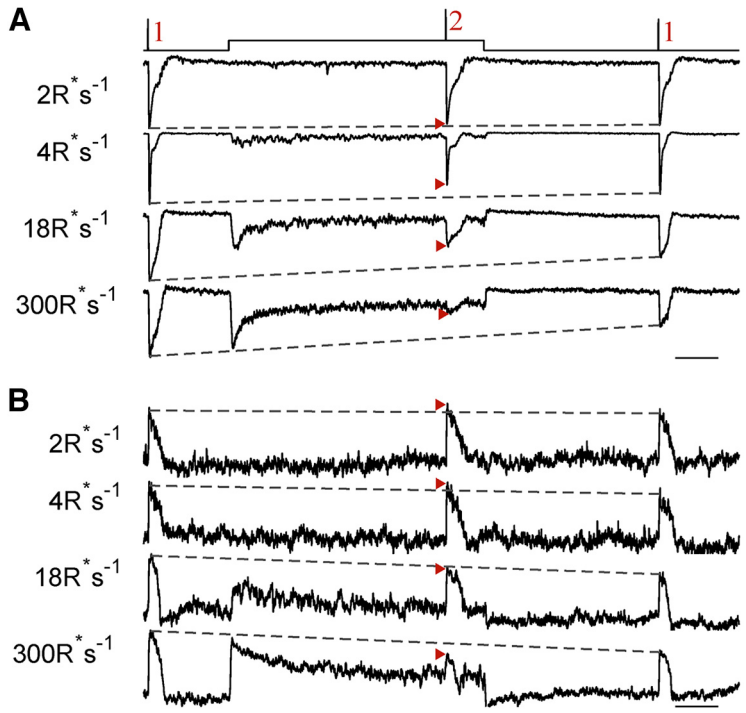

Figure 5. RBC maximal response is attenuated in background light. ***A***, Representative current responses of RBCs were recorded in voltage clamp (Vm = −60 mV) to saturating flashes of light that were delivered during the presentation of a background light (2, red), bracketed by saturating flashes in darkness (1, red). Top, The stimulus monitor. To account for cellular rundown, a linear trend was computed from the maximal response peaks in darkness (dashed line), and the maximal response amplitudes during background illumination were calculated relative to their expected maximum (indicated by red right-facing arrowheads). Intensities of flashes in darkness (1, red) were 20–30 R*. Flashes delivered during background illumination (2, red) were 20–1000 R* and were scaled with the background intensity to ensure a saturated response (Table 1, intensity ranges). Increased background light resulted in larger decreases of the saturating-light response. ***B***, Representative current responses from RBCs as in ***A***, with the addition of 10 mM BAPTA to the recording pipette and at a holding potential of Vm = +50 mV. Under these conditions, dim and moderate background illumination had little effect on the saturating-light response. Responses in ***A*** and ***B*** were scaled by the peak of the first response of each trace.

negligible at these light intensities (Fig. 1*B*; Dunn et al., 2006; Morshedian et al., 2018).

In brighter backgrounds, attenuation rapidly increased before tapering off around $R_{max}/\hat{R}_{max}$ = 0.61 (0.56, 0. 67) [ΔR = 0.31 (0.26, 0.31)]. In the brightest background we tested (400 R* s^{-1}), the attenuation reached below 0.5, which corresponded to a peak amplitude of −18 (−37, −11) pA. The inflection point of the model, that is, the background level producing half-maximal attenuation calculated from Equation 2, was $I^B_{1/2}$ = 6.0 (2.9, 7.9) R* s^{-1}, which is well below the I_0 of 53 R* s^{-1} for rods (the background intensity decreasing rod sensitivity by a factor of two; Fig. 1*B*).

The decrease in R_{max} in dim backgrounds requires Ca^{2+} entry

Because the decrease in R_{max} could occur at backgrounds too dim to elicit significant adaptation of the rods (Fig. 1*B*), the process producing this effect must be occurring within the bipolar cells. To test for an effect of Ca^{2+} on the decrease in R_{max}, we therefore recorded responses to saturating flashes in darkness and in backgrounds with the membrane potential clamped to +50 mV (Nawy, 1999) and with 10 mM BAPTA in the recording pipette (Fig. 5*B*). This combination minimizes changes in intracellular Ca^{2+} by decreasing Ca^{2+} entry and increasing intracellular buffering. Current deflections are outward oriented because the holding potential was near the reversal potential of Na^+ (Nernst potential of +56 mV for our solutions). The outward current was probably carried predominantly by K^+ efflux.

Using the same protocol and analysis as described earlier (Fig. 5*A*), we found that the average of peak responses met or slightly exceeded predicted maxima in background levels less than ∼10 R* s^{-1} (Fig. 5*B*), indicating that R_{max} was unaffected at these dim background intensities (p = 0.29). Consistent with previous reports (Berntson et al., 2004), we found that inclusion of BAPTA in the recording pipette together with a holding potential of +50 mV nearly abolished the rapid transient decay at the onset of the background step. Brighter backgrounds still elicited a slower component of decay that reached a plateau of 45 (35, 56)% of the maximal response peak in darkness. In control conditions at a background intensity producing ∼300 R* s^{-1}, the plateau reached 27 (21, 35)% of the maximal response peak in darkness. Hence, BAPTA significantly decreased the decay of the step response (p = 0.049).

To compare the effects of Ca^{2+} on the suppression of R_{max}, we calculated $R_{max}/\hat{R}_{max}$ as a function of background intensities but in experiments with V_m = +50 mV and with BAPTA in the pipette (Fig. 6, red symbols and line). The background intensity was again related to the fractional suppression of R_{max} by fitting with an inverse Hill equation. From these fits, we found that $I^B_{1/2}$ shifted significantly to brighter light intensities compared with control conditions [$I^B_{1/2}$= 33 (16, 50) R* s^{-1}; $p < 0.05$ by 95% CI comparison]. Concomitantly, the initial offset parameter R_0 in Equation 2 was significantly higher in the Ca^{2+}-buffered condition [R_0 = 1.0 (0.99, 1.1) vs R_0 = 0.92 (0.88, 0.95) in control condition, $p < 0.05$ by 95% CI comparison]. The value of R_0 can be visualized to the left in Figure 6 as the apparent plateau of the red and black curves at the dimmest intensities. The black curve seems to intercept the y-axis at a lower value of R_{max}, although there is no true intercept because intensities are plotted on a log scale, and $R_{max}/\hat{R}_{max}$ is one when the background intensity is zero (by definition). To confirm this difference in R_0, we performed a repeated-measures ANOVA on the fractional R_{max} suppression measurements over the lowest six background levels and found a significant effect of Ca^{2+} buffering (p = 0.00,015), as well as a significant interaction between background level and Ca^{2+} buffering (p = 0.0002). That R_0 is less in the control condition indicates that there is some effect of Ca^{2+} on R_{max} at the dimmest background intensities we used in our experiments and perhaps even in dimmer light.

The decrease in R_{max} is not produced by a change in single-channel conductance

One possible explanation of the effect of background light is a change in the single-channel conductance of the TRPM1 channel. To determine whether TRPM1 conductance is affected by background light, we estimated single-channel currents with

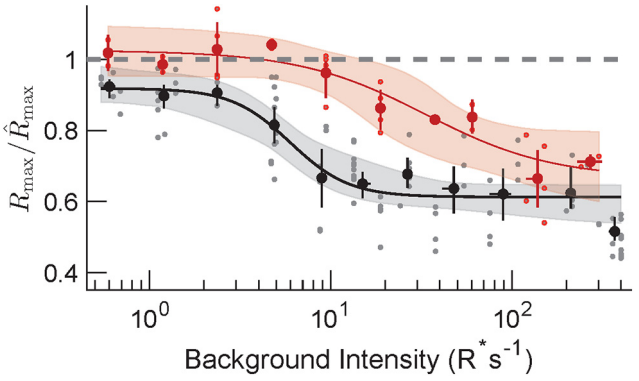

Figure 6. Calcium entry during light exposure modulates the maximal response amplitude. Relative change in R_{max} from darkness as a function of background intensity for control conditions (black; Vm = −60 mV; normal internal) and Ca^{2+}-buffered conditions (red; Vm = +50 mV; 10 mM BAPTA internal). Peak responses, $\hat{R}_{max}$, from experiments described in Figure 5 were scaled by the predicted maximal response, $\hat{R}_{max}$. Dim background levels (less than ∼10 $R^*\ s^{-1}$) yielded responses that were sometimes larger than predicted (dashed line) in the Ca^{2+}-buffered condition. The relationship of fractional change versus background intensity for the Ca^{2+}-buffered condition appeared shifted upward and rightward, with significant changes in two fitted parameters, R_0 = 1.0 (0.99,1.1; $p < 0.05$) and $I^{\beta}_{1/2}$ = 33 (16, 50) $R^*\ s^{-1}$ ($p < 0.05$), compared with R_0 = 0.92 (0.88, 0.95) and $I^{\beta}_{1/2}$ = 6.0 (2.9, 7.8) $R^*\ s^{-1}$ ($p < 0.05$) for control conditions. Other fitted parameters were as follows: ΔR = 0.31 (0.26, 0.31) and n = 2.7 (1.4, 3.0) for control and ΔR = 0.36 (0.22, 0.42) and n = 1.2 (0.65, 1.7) for Ca^{2+}-buffered conditions.

nonstationary noise analysis (Sampath and Rieke, 2004; Hartveit and Veruki, 2007) in darkness and in background light (Fig. 7*A*). We found no differences in single-channel currents at the backgrounds tested (levels below 35 $R^*\ s^{-1}$, ANOVA p = 0.56). Single-channel currents were estimated to be 0.27 (0.24, 0.34) pA in darkness and between 0.10 and 0.52 pA across all backgrounds tested (Fig. 7*B*). These values agree with previous reports in darkness (0.27 pA in Sampath and Rieke, 2004). From parabolic fits (Hartveit and Veruki, 2007); we estimated the log-fold change in the number of open channels from the steady state before the flash and from the falling phase of the maximal response (Fig. 7*C*). We found that background light produced a significant reduction of log-fold change in open channels [−2.6 (−3.3, −1.8) in 24 $R^*\ s^{-1}$ compared with darkness; p = 0.0001]. Thus, brighter background light likely leads to a reduction in the number of channels that are available to open but does not affect the single-channel conductance.

Discussion

We have studied mechanisms of adaptation in mouse retina by making patch-clamp recordings from rods and RBCs in retinal slices in darkness and in background illumination. We characterized changes in RBC responses from the three parameters of the Hill equation, that is, flash sensitivity from $I_{1/2}$ (intensity at half-maximal response), response-intensity nonlinearity from n, and maximal response amplitude from R_{max}. Our experiments indicate three separate effects of background light on RBCs, namely, a decrease in sensitivity reflected in the increase of $I_{1/2}$ (Fig. 3*B*), a reduction in the slope of the response-intensity curve reflected by a decrease in n (Fig. 2*C*), and a surprising decrease in the maximum amplitude of response R_{max}. These three effects are likely to be at least in part independent. The decrease in RBC sensitivity in background light occurs only in light bright enough to adapt the rods and is derived directly from the decrease in rod sensitivity (Fig. 3*B*). The change in the slope of the response-intensity curve occurs at intensities too dim to produce adaptation in rods and is already complete in a background intensity of ∼2-5 $Rh^*\ rod^{-1}\ s^{-1}$ (Fig. 3*A*). The decrease in R_{max} also occurs at intensities too dim to produce adaptation in the rods but continues to be significant in a range of light intensities brighter than those responsible for the change in n (Figs. 5, 6). The effect on R_{max} indicates that sustained illumination desensitizes the RBC transduction cascade or produces a change in the conformation of the TRPM1 channels so that they somehow become reluctant to open (Bean, 1989) without a change in their unitary conductance (Fig. 7). Modulation of n and R_{max} are both likely to be produced by regulation of some step in the RBC transduction cascade by Ca^{2+} as both are affected by holding the membrane potential at a positive value and/or dialysis of BAPTA (Figs. 4, 5).

Modulation of $I_{1/2}$

The sensitivity of RBCs could not be measured as for rods from small-amplitude responses because this method assumes linearity—true for rods but not for dark-adapted RBCs or in dim background light (Figs. 2*C*, 3*A*). On the assumption that the inverse of $I_{1/2}$ is a measure of the sensitivity of the cell (S_f), we compared the change in relative sensitivity in background light for rods and RBCs and show that these relationships are indistinguishable (Fig. 3*B*). Although RBCs pool rod signals and are more sensitive than single rods, the relative changes in sensitivity produced by background light are practically the same. We conclude that the adaptation of RBC sensitivity is derived directly from adaptation of sensitivity in rods without further synaptic modulation. Our finding for rods agrees with previous measurements of Dunn et al. (2007) for cones, who demonstrated a similar relationship between cones and cone bipolar cells.

Modulation of n

Previous experiments have shown that the response-intensity curve for dark-adapted RBCs is nonlinear, with a Hill coefficient of 1.4–1.7 (Field and Rieke, 2002; Berntson et al., 2004; Sampath and Rieke, 2004). This steepness of the response-intensity curve in darkness allows the synapse to distinguish more easily between small responses that are probably noise from larger responses that are more likely to be driven by light (Van Rossum and Smith, 1998). In the presence of background light, this nonlinearity disappears (Figs. 2C, 3*A*; Sampath and Rieke, 2004). In brighter illumination, it may be less important to distinguish small-amplitude signals and more useful to preserve a greater range of responsiveness across a larger range of stimuli.

The nonlinearity in dark-adapted RBCs cannot derive from the signals of rods as rod response amplitude increases linearly with stimulus intensity (Field and Rieke, 2002); the Hill coefficient n for rods is close to 1.0. The nonlinearity in dark-adapted RBCs must therefore arise from some feature of synaptic transmission. Our experiments demonstrate that the nonlinearity decreases in background light but becomes even steeper when the solution of the recording pipette contains the Ca^{2+} buffer BAPTA (Fig. 4; Berntson et al., 2004), suggesting the following hypothesis. In dark-adapted RBCs, glutamate release from rods activates the RBC signal-transduction cascade holding TRPM1 channels mostly closed (Sampath and Rieke, 2004). TRPM1 channels are nonselective cationic and permeable to Ca^{2+} (Oancea and Wicks, 2011), but as they are closed in darkness, the free-Ca^{2+} concentration in RBC dendrites should be low. In background light as the channels start to open, the free-Ca^{2+} concentration would rise, and this increase in Ca^{2+} may reduce

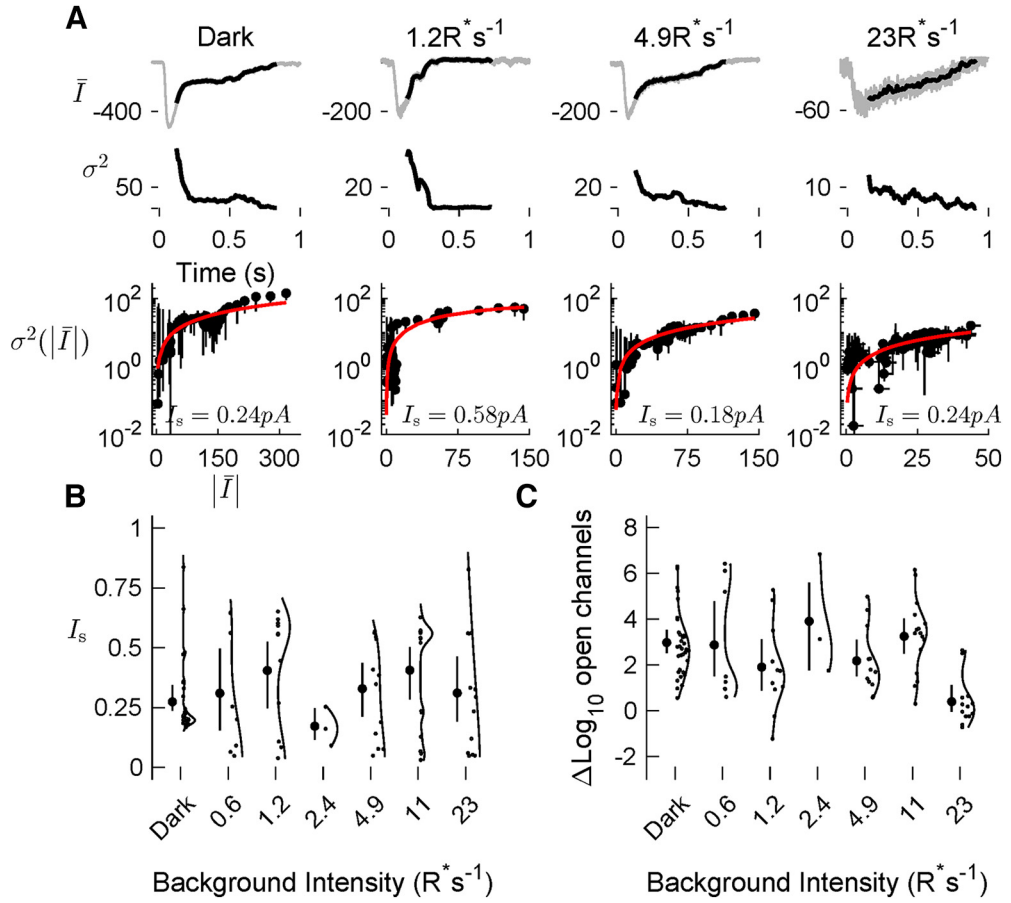

Figure 7. Nonstationary noise analysis of single-channel currents. ***A***, Representative current responses, variance, and nonstationary noise fits in darkness, 1.2, 4.9, and 23 $R^* s^{-1}$. Responses were binned into 10 ms windows 20–50 ms following the peak of the response, and the mean (I, top) and variance (σ^2, middle) were calculated for each bin. The analysis region of the variance was plotted as a function of the absolute value of the mean bins below. To estimate the single-channel current I_s and the number of open channels at the peak of the response *N*, the data were fit with the following equation (red trace): $\sigma^2(|\bar{I}|) = I_s|\bar{I}| - |\bar{I}|^2/N + \sigma_0^2$, where σ_0^2 is the baseline variance. ***B***, Single-channel current estimates. ***C***, Log-fold change in the estimated number of channels open at the peak (*N*) relative to the steady-state point 200 ms before the flash delivery as calculated as $log_{10}(N - \sigma_0^2/I_s^2)/\sigma_0^2/I_s^2$.

nonlinearity of the response-intensity relationship. If RBCs are dialyzed with the nanomolar-affinity Ca^{2+} chelator BAPTA from the recording pipette, the buffering of Ca^{2+} in the RBC may further reduce the effective concentration of Ca^{2+} in the vicinity of the synapse, and the nonlinearity could then increase (Fig. 4). Although BAPTA would not alter the steady-state concentration of Ca^{2+} throughout the RBC, it could alter local and time-dependent changes in concentration. We hypothesize that Ca^{2+} has some effect on the synaptic transduction cascade of the RBC, perhaps near the site of Ca^{2+} entry in the vicinity of the TRPM1 channels.

Ultimately the dark glutamate release rate sets the extent of RBC nonlinearity. Although postsynaptic mGluR6 receptors are not saturated in darkness (Sampath and Rieke, 2004), their relative occupancy may play a critical role in saturation of the signaling cascade. Previous work has shown that mGluR dimers display a nonlinear increase in transduction efficiency when both subunits bind glutamate (Levitz et al., 2016). A possible explanation for RBC nonlinearity is that in darkness synaptic glutamate rests at a level where the mGluR6 dimers are straddling the singly and doubly liganded state. This interpretation is supported by the linearization of the rod bipolar-cell response-intensity relationship by weak background light (Fig. 3) or by application of a low concentration of a high-affinity antagonist of the mGluR6 receptors (Sampath and Rieke, 2004).

Modulation of R_{max}

We show that R_{max}, the maximum amplitude of the RBC flash response, is markedly decreased by background light even at intensities too dim to produce adaptation in rods. Moreover, this effect is greatly reduced when the Ca^{2+} concentration is prevented from changing by a combination of infusion of BAPTA and a holding potential of +50 mV. An increase in Ca^{2+} in RBC dendrites appears to be producing some change in the transduction cascade or in the TRPM1 channels so that the channels are prevented from opening to their maximal extent but without changing their single-channel conductance (Fig. 7). There could be a Ca^{2+}-dependent effect on $G\alpha_o$ that prevents it from deactivating as much as in a dark-adapted cell or an alteration of the rate of production or destruction of the second messenger of the cascade, whose identity is presently unknown. Alternatively, the TRPM1 channels could transiently enter a conformational state in which they are reluctant to open, much as Bean (1989) showed for neuronal Ca^{2+} channels modulated by $G\beta\gamma$.

As in previous reports, we also found that RBC responses to bright light had a characteristic transient peak followed by a rapid sag toward a plateau, which was also eliminated by impeding Ca^{2+} entry (Fig. 5; Berntson et al., 2004). This effect seems to be produced by Ca^{2+}, perhaps by binding to the TRPM1 channels (Berntson et al., 2004). Ca^{2+} entering the RBC during presentation of steady illumination could first inhibit opening of the

TRPM1 channels as Berntson et al. (2004) suggested, then cause the channels to move slowly into a conformational state that prevents them from opening to their fullest extent. If so, the entry and departure from this state must occur rapidly to explain the time course of the changes we have observed (Fig. 5*A*). Such effects might occur with a Ca^{2+}-binding site near the channel pore, as has been observed with other members of the TRPM family (Winkler et al., 2017). Further studies of this effect may give additional details about its mechanism and its relationship to the production of the transient peak and rapid decay of the response.

Adaptation to background light in rod bipolar cells

Adaptation is known to operate on many time scales to provide a robust scaling of sensitivity with changing background light. Adaptational effects studied here were characterized on fast time scales following the delivery of background light, but additional mechanisms may contribute to adaptation on longer time scales of 10+ min. These include potential sensitizing effects of cGMP through protein kinase G (Snellman and Nawy, 2004) but also desensitizing effects independent of cGMP by Ca^{2+}/calmodulin-dependent protein kinase II (Walters et al., 1998; Shiells and Falk, 2000) and the Ca^{2+}-dependent phosphatase calcineurin (Snellman and Nawy, 2002). How these mechanisms collectively operate to provide a seamless representation of light intensity as luminance increases remains an open question.

Our experiments provide a comprehensive investigation of the fast effects of background light on mammalian RBCs. These cells synapse onto AII amacrine cells, which convey the rod signals to cone bipolar cells and then to ganglion cells (Fain and Sampath, 2018). It seems likely that rod signals undergo further adaptation downstream in the retina because adaptation of scotopic vision can occur at light intensities even dimmer than those we have used in our experiments (Rushton, 1965), probably in cells pooling an even larger number of rod responses (Dunn and Rieke, 2008). Our work on RBCs should provide the basis of further investigation at more proximal sites in the retina, to discover how adaptation proceeds for rod signals over the whole range of illumination of scotopic vision.

References

Arman AC, Sampath AP (2010) Patch clamp recordings from mouse retinal neurons in a dark-adapted slice preparation. J Vis Exp 2010:2107.

Baylor DA, Lamb TD, Yau K (1979) Responses of retinal rods to single photons. J Physiol 288:613–634.

Bean BP (1989) Neurotransmitter inhibition of neuronal calcium currents by changes in channel voltage dependence. Nature 340:153–156.

Benjamini Y, Hochberg Y (1995) Controlling the false discovery rate: a practical and powerful approach to multiple testing. J R Stat Soc Ser B Methodol 57:289–300.

Berntson A, Smith RG, Taylor WR (2004) Postsynaptic calcium feedback between rods and rod bipolar cells in the mouse retina. Vis Neurosci 21:913–924.

Cao Y, Pahlberg J, Sarria I, Kamasawa N, Sampath AP, Martemyanov KA (2012) Regulators of G protein signaling RGS7 and RGS11 determine the onset of the light response in ON bipolar neurons. Proc Natl Acad Sci U S A 109:7905–7910.

Chang B, Hawes NL, Hurd RE, Davisson MT, Nusinowitz S, Heckenlively JR (2002) Retinal degeneration mutants in the mouse. Vision Res 42:517–525.

Chen C-K, Burns ME, He W, Wensel TG, Baylor DA, Simon MI (2000) Slowed recovery of rod photoresponse in mice lacking the GTPase accelerating protein RGS9-1. Nature 403:557–560.

Chen C-K, Woodruff ML, Chen FS, Chen D, Fain GL (2010) Background light produces a recoverin-dependent modulation of activated-rhodopsin lifetime in mouse rods. J Neurosci 30:1213–1220.

Dhingra A, Lyubarsky A, Jiang M, Pugh EN, Birnbaumer L, Sterling P, Vardi N (2000) The light response of ON bipolar neurons requires G[aloha]o. J Neurosci 20:9053–9058.

Dunn FA, Rieke F (2008) Single-photon absorptions evoke synaptic depression in the retina to extend the operational range of rod vision. Neuron 57:894–904.

Dunn FA, Doan T, Sampath AP, Rieke F (2006) Controlling the gain of rod-mediated signals in the mammalian retina. J Neurosci 26:3959–3970.

Dunn FA, Lankheet MJ, Rieke F (2007) Light adaptation in cone vision involves switching between receptor and post-receptor sites. Nature 449:603–606.

Efron B (1987) Better bootstrap confidence intervals. J Am Stat Assoc 82:171–185.

Efron B, Tibshirani R (1986) Bootstrap methods for standard errors, confidence intervals, and other measures of statistical accuracy. Stat Sci 1:54–75.

Fain G, Sampath AP (2018) Rod and cone interactions in the retina. F1000Res 7:657.

Field GD, Rieke F (2002) Nonlinear signal transfer from mouse rods to bipolar cells and implications for visual sensitivity. Neuron 34:773–785.

Frederiksen R, Morshedian A, Tripathy SA, Xu T, Travis GH, Fain GL, Sampath AP (2021) Rod photoreceptors avoid saturation in bright light by the movement of the G protein transducin. J Neurosci 41:3320–3330.

Freedman DA (1981) Bootstrapping regression models. Ann Stat 9:1218–1228.

Govardovskii VI, Fyhrquist N, Reuter T, Kuzmin DG, Donner K (2000) In search of the visual pigment template. Vis Neurosci 17:509–528.

Hartveit E, Veruki ML (2007) Studying properties of neurotransmitter receptors by non-stationary noise analysis of spontaneous postsynaptic currents and agonist-evoked responses in outside-out patches. Nat Protoc 2:434–448.

Hecht S, Shlaer S, Pirenne MH (1941) Energy at the threshold of vision. Science 93:585–587.

Ingram NT, Sampath AP, Fain GL (2019) Voltage-clamp recordings of light responses from wild-type and mutant mouse cone photoreceptors. J Gen Physiol 151:1287–1299.

Kaur T, Nawy S (2012) Characterization of Trpm1 desensitization in ON bipolar cells and its role in downstream signalling. J Physiol 590:179–192.

Levitz J, Habrian C, Bharill S, Fu Z, Vafabakhsh R, Isacoff EY (2016) Mechanism of assembly and cooperativity of homomeric and heteromeric metabotropic glutamate receptors. Neuron 92:143–159.

Makino CL, Dodd RL, Chen J, Burns ME, Roca A, Simon MI, Baylor DA (2004) Recoverin regulates light-dependent phosphodiesterase activity in retinal rods. J Gen Physiol 123:729–741.

Mendez A, Burns ME, Sokal I, Dizhoor AM, Baehr W, Palczewski K, Baylor DA, Chen J (2001) Role of guanylate cyclase-activating proteins (GCAPs) in setting the flash sensitivity of rod photoreceptors. Proc Natl Acad Sci U S A 98:9948–9953.

Morgans CW, Zhang J, Jeffrey BG, Nelson SM, Burke NS, Duvoisin RM, Brown RL (2009) TRPM1 is required for the depolarizing light response in retinal ON-bipolar cells. Proc Natl Acad Sci U S A 106:19174–19178.

Morshedian A, Fain GL (2017) Light adaptation and the evolution of vertebrate photoreceptors. J Physiol 595:4947–4960.

Morshedian A, Woodruff ML, Fain GL (2018) Role of recoverin in rod photoreceptor light adaptation: recoverin and light adaptation. J Physiol 596:1513–1526.

Nawy S (1999) The metabotropic receptor mGluR6 may signal through G(o), but not phosphodiesterase, in retinal bipolar cells. J Neurosci 19:2938–2944.

Nawy S (2000) Regulation of the on bipolar cell mGluR6 pathway by Ca 2+. J Neurosci 20:4471–4479.

Nawy S (2004) Desensitization of the mGluR6 transduction current in tiger salamander On bipolar cells. J Physiol 558:137–146.

Neher E (1992) Correction for liquid junction potentials in patch clamp experiments. Methods Enzymol 207:123–131.

Nymark S, Frederiksen R, Woodruff ML, Cornwall MC, Fain GL (2012) Bleaching of mouse rods: microspectrophotometry and suction-electrode recording. J Physiol 590:2353–2364.

Oancea E, Wicks NL (2011) TRPM1: New trends for an old TRP. In: Transient receptor potential channels (Islam MS, ed), pp 135–145. New York: Springer.

Okawa H, Miyagishima KJ, Arman AC, Hurley JB, Field GD, Sampath AP (2010a) Optimal processing of photoreceptor signals is required to maximize behavioural sensitivity. J Physiol 588:1947–1960.

Okawa H, Pahlberg J, Rieke F, Birnbaumer L, Sampath AP (2010b) Coordinated control of sensitivity by two splice variants of Gα(o) in retinal ON bipolar cells. J Gen Physiol 136:443–454.

Petráš I, Bednárová D (2010) Total least squares approach to modeling: a Matlab toolbox. Acta Montan Slovaca 15:158–170.

Rushton WA (1965) The Ferrier lecture, 1962 visual adaptation. Proc R Soc Lond.B Biol Sci 162:20–46.

Sampath AP, Rieke F (2004) Selective transmission of single photon responses by saturation at the rod-to-rod bipolar synapse. Neuron 41:431–443.

Sherman AJ, Shrier A, Cooper E (1999) Series resistance compensation for whole-cell patch-clamp studies using a membrane state estimator. Biophys J 77:2590–2601.

Shiells RA, Falk G (1999) A rise in intracellular Ca2+ underlies light adaptation in dogfish retinal "on" bipolar cells. J. Physiol 514:343–350.

Shiells RA, Falk G (2000) Activation of Ca2+–calmodulin kinase II induces desensitization by background light in dogfish retinal 'on' bipolar cells. J Physiol 528:327–338.

Snellman J, Nawy S (2002) Regulation of the retinal bipolar cell mGluR6 pathway by calciuneurin. J Neurophysiol 88:1088–1096.

Snellman J, Nawy S (2004) cGMP-dependent kinase regulates response sensitivity of the mouse on bipolar cell. J Neurosci 24:6621–6628.

Tikidji-Hamburyan A, Reinhard K, Seitter H, Hovhannisyan A, Procyk CA, Allen AE, Schenk M, Lucas RJ, Münch TA (2015) Retinal output changes qualitatively with every change in ambient illuminance. Nat Neurosci 18:66–74.

Tsukamoto Y, Morigiwa K, Ueda M, Sterling P (2001) Microcircuits for night vision in mouse retina. J Neurosci 21:8616–8623.

van der Velden HA (1946) The number of quanta necessary for the perception of light of the human eye. Ophthalmologica 111:321–331.

van Rossum MC, Smith RG (1998) Noise removal at the rod synapse of the mammalian retina. Vis Neurosci 15:809–821.

Walters RJ, Kramer RH, Nawy S (1998) Regulation of cGMP-dependent current in On bipolar cells by calcium/calmodulin-dependent kinase. Vis Neurosci 15:257–261.

Welch BL (1938) The significance of the difference between two means when the population variances are unequal. Biometrika 29:350–362.

Welch BL (1947) The generalisation of student's problems when several different population variances are involved. Biometrika 34:28–35.

Winkler PA, Huang Y, Sun W, Du J, Lü W (2017) Electron cryo-microscopy structure of a human TRPM4 channel. Nature 552:200–204.

Woodruff ML, Janisch KM, Peshenko IV, Dizhoor AM, Tsang SH, Fain GL (2008) Modulation of phosphodiesterase6 turnoff during background illumination in mouse rod photoreceptors. J Neurosci 28:2064–2074.